Impact-parameter-dependent multifragmentation of C_{60} in charge-changing collisions with 2-MeV C^+ ions

T. Mizuno,[1] D. Okamoto,[1] T. Majima,[2] Y. Nakai,[3] H. Tsuchida,[1] and A. Itoh[1,*]
[1]*Department of Nuclear Engineering, Kyoto University, Kyoto 606-8501, Japan*
[2]*Genesis Research Institute, Inc., Ichikawa 272-0001, Japan*
[3]*RIKEN (The Institute of Physical and Chemical Research), Wako, Saitama 351-0198, Japan*
(Received 27 March 2007; published 15 June 2007)

Multifragmentation of C_{60} was investigated for 2 MeV C^+ projectile ions by means of a time-of-flight triple coincidence technique. Fragment ions and secondary electrons were measured simultaneously in coincident with charge-selected outgoing projectile particles scattered into forward angles smaller than 1.0 mrad. Fragment ion distributions were found to change remarkably with respect to the scattering angle θ. Relationships between θ and the impact parameter b measured from the center of C_{60} were calculated classically. We found evidently that small-size fragment ions are produced only from cage-penetration collisions, while intact parent ions and their daughter ions are created in collisions nearby but outside a C_{60}. Furthermore, charge state distributions of prefragmented C_{60}^{r+} ions and correlated fragment ion pairs were both found to be essentially independent of θ when plotted for individual C_m^+ ions of fixed size. These results indicate that the production of a size-fixed specific ion may be restricted to a certain impact parameter region in which equivalent electronic energies are deposited irrespectively of θ. This was confirmed also from our calculation of the energy deposition as a function of b carried out using the local density approximation.

DOI: 10.1103/PhysRevA.75.063203 PACS number(s): 36.40.Qv

I. INTRODUCTION

In the past decade, fullerene molecules have attracted considerable attention as a collision partner providing information about properties of matter lying between atoms and solids [1]. Among many experimental results on ionization and fragmentation of C_{60} obtained to date by various primary probes of charged particles and photons [1–18], it is noteworthy that the C_{60} molecule has remarkable high stability against Coulomb repulsive force. For instance, evidence for the existence of highly ionized intact ions like a C_{60}^{12+} is reported in recent experimental work using an intensive femtosecond laser [4]. On the other hand, charged particle bombardment on C_{60} tends to result in molecular fragmentation arising from instability due to Coulomb repulsive force and to internal excitation energy. The former mechanism is important in collisions with slow highly charged ions (SHCI), since multiply charged prefragmented ions C_{60}^{r+} are easily produced via multiple electron capture taking place at rather large impact parameters [6]. In such collisions, the internal excitation energy is supposed to be small. The latter mechanism, i.e., instability due to high internal excitation, becomes significant in fast ion collisions, where a large amount of inelastic energy E_d is deposited into a C_{60} [7–18]. As the total amount of E_d is supposed to depend on the impact parameter b between collision partners, it is important to know the relationship between E_d and b. Nevertheless, no such investigations have been carried out so far except for SHCI experiments [19–23] of scattering angle dependent electron capture collisions. Among these investigations, Cederquist *et al.* discussed in detail the relationship between fragmentation and b [23].

In the present work, fast ion induced C_{60}-multifragmentation is investigated at scattering angles from 0 to 1.0 mrad. At each scattering angle we carried out simultaneous measurements of fragment ions, the number of secondary electrons, and charge-selected outgoing projectile particles. This triple coincidence technique allows us to obtain information about (i) correlation between fragment ion pairs and (ii) r distributions of C_{60}^{r+} in correlation with a C_m^+ ion of any cluster size m. As the scattering angle θ is closely related to the impact parameter b in collisions, all the θ-dependent data can be interpreted in terms of b as described in the following sections.

II. EXPERIMENT

The experiment was performed at the QSEC heavy ion facility of Kyoto University. The experimental method and apparatus are described elsewhere [14,16,17], so that only a brief outline is given below.

A beam of 2.0 MeV C^+ ions provided from a 1.7 MV tandem accelerator was carefully collimated to smaller than 0.1 mm in diameter by two-dimensional knife-edged slits and was charge purified with a magnetic charge-selector before entering a collision chamber. A gas phase C_{60} target was produced by sublimation of high-purity (99.98%) powder at 550 °C. A base pressure of the target chamber was kept below 5×10^{-6} Pa. After collisions with the C_{60} target, outgoing projectiles were charge separated horizontally by an electrostatic deflector and detected by a movable semiconductor detector (SSD) located 1 m downstream of the collision chamber. The scattering angle θ was resolved by placing a hole slit of 0.5 mm in diameter in front of the SSD. An acceptance angle of the detector was 0.5 mrad.

Positive fragment ions and secondary electrons were extracted into opposite directions by an electric field of

*Electronic address: itoh@nucleng.kyoto-u.ac.jp

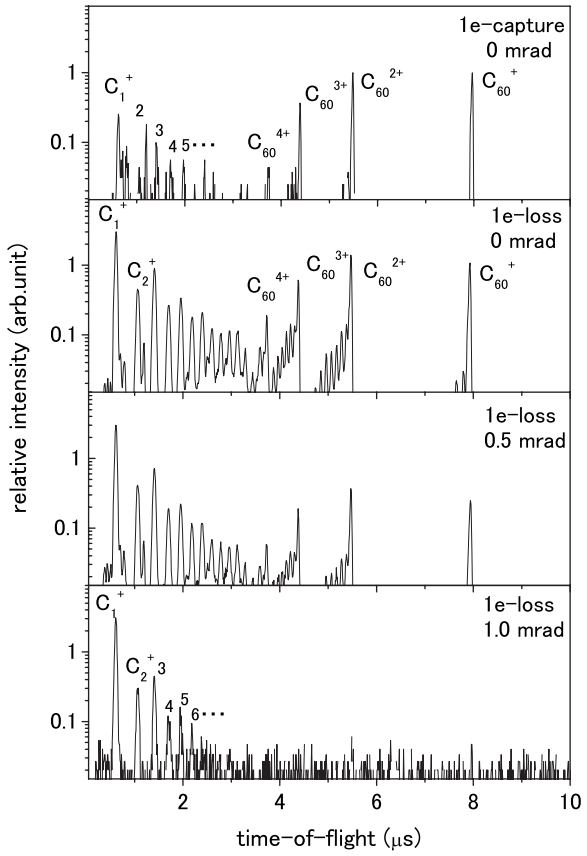

FIG. 1. Time-of-flight spectra of fragment ions produced in 1*e*-capture and 1*e*-loss collisions of 2 MeV C^+ measured at scattering angles of θ=0, 0.5, and 1.0 mrad.

615 V/cm applied perpendicular to the incident beam axis. Fragment ions were detected by a two-stage multichannel plate with a front voltage of −4.6 kV. The mass distribution of product ions was measured by a time-of-flight method. Secondary electrons were detected by a PIPS type detector biased at +30 kV, enabling us to obtain the number of secondary electrons n_e emitted simultaneously. Detection of fragment ions and secondary electrons was carried out in coincidence with charge-and-scattering angle resolved scattered ions. We applied this triple coincidence technique to single electron loss and capture collisions.

III. RESULTS AND DISCUSSION

Figure 1 shows time-of-flight spectra of fragment ions measured for single electron capture (1*e*-capture) and single electron loss (1*e*-loss) collisions of 2.0 MeV C^+ with C_{60}. Data were taken at three scattering angles of $\theta=0\pm0.25$, 0.5 ± 0.25, and 1.0 ± 0.25 mrad. It was found that 1*e*-capture events were considerably smaller than 1*e*-loss and the difference was more than two orders of magnitude. Also, in 1*e*-capture collisions almost no peak intensities were found at θ=0.5 and 1.0 mrad. One can see that spectral profiles in 1*e*-loss collisions change remarkably depending on the scattering angle. Ionized parent ions C_{60}^{r+} and their fullerenelike daughter ions decrease rapidly as θ increases and they nearly vanish at 1.0 mrad.

In order to know the relationship between the scattering angle θ and the impact parameter b measured from the center of C_{60}, a simulation calculation has been done as follows. The calculation was performed for 100 000 incident particles with randomly generated projectile positions (x,y) with $x^2+y^2=b^2$, where the plane (x,y) is perpendicular to the incident beam direction. Molecular orientation of C_{60} was also generated randomly with respect to the incident beam direction. For each value of b impact parameters p's between the incident ion and 60 carbon atoms were calculated individually. Here we calculated only binary collisions between the incident ion and the closest carbon atom because multiple collision events inside C_{60} are negligibly small. Furthermore, we restricted our calculation to a range of $p\leqslant4$, corresponding to about twice the atomic carbon radius [24], since electron loss and capture collisions are unlikely to occur at $p>4$ in fast collisions [25]. The scattering angle Θ in the center-of mass (c.m.) frame was calculated classically as

$$\Theta=\pi-2p\int_{r_c}^{\infty}r^{-2}\left(1-\frac{p^2}{r^2}-\frac{V(r)}{E_{\mathrm{c.m.}}}\right)^{-1/2}dr, \qquad (1)$$

where r is the internuclear distance, p the impact parameter, $E_{\mathrm{c.m.}}$ the incident energy in the c.m. frame, r_c the closest approach distance, and $V(r)$ the interaction potential for which we used the ZBL-type universal potential [26]. As the collision partners are identical and an inelastic energy loss is estimated to be negligibly small compared to the incident energy [27], the scattering angle θ in the laboratory frame is approximated by $\theta=\Theta/2$.

Calculated yields of scattering into θ=0, 0.5, and 1.0 mrad are plotted in Fig. 2 as a function of b. The number density of target carbon atoms is also depicted in the upper figure. It is found that scattering into none-zero angles ($\theta\neq0$) is essentially limited to $b\leqslant7$, i.e., cage penetration collisions. Together with the results from Fig. 1, we find that small fragment ions like $C_{1,2,3}^+$ are produced in these cage penetration collisions, while parent ions C_{60}^{r+} are produced outside or in a peripheral area of C_{60}.

Present results coincide reasonably with those obtained in SHCI experiments [5,6]. In our fast ion collisions, fission into two charged fragment ions such as $C_{60}^{4+}\rightarrow C_{58}^{3+}+C_2^+$ was found to occur scarcely and multifragmentation is dominant. Examples of emission distributions of fragment ions correlated with C_1^+ and C_3^+ are shown in Fig. 3. One can see that the fragment yields decrease with increasing number of carbon atoms, and, as expected, the yield correlated with C_1^+ decreases more rapidly in comparison with C_3^+. An important result is that the fragment distribution is less sensitive to the scattering angle.

Figure 4 shows charge state distributions of prefragmented C_{60}^{r+} ions obtained for fixed-sized fragment ions of C_n^+ (n=1,3,5). The r-distribution shows again almost the same profiles independently of the scattering angles. For comparison, data obtained for C_1^+ in 1*e*-capture collisions at θ=0 are also plotted in the uppermost figure. One can see that the distribution profile is also the same as 1*e*-loss collisions. Present results of θ-independency both for mass distributions (Fig. 3) and r-distributions indicate clearly that a

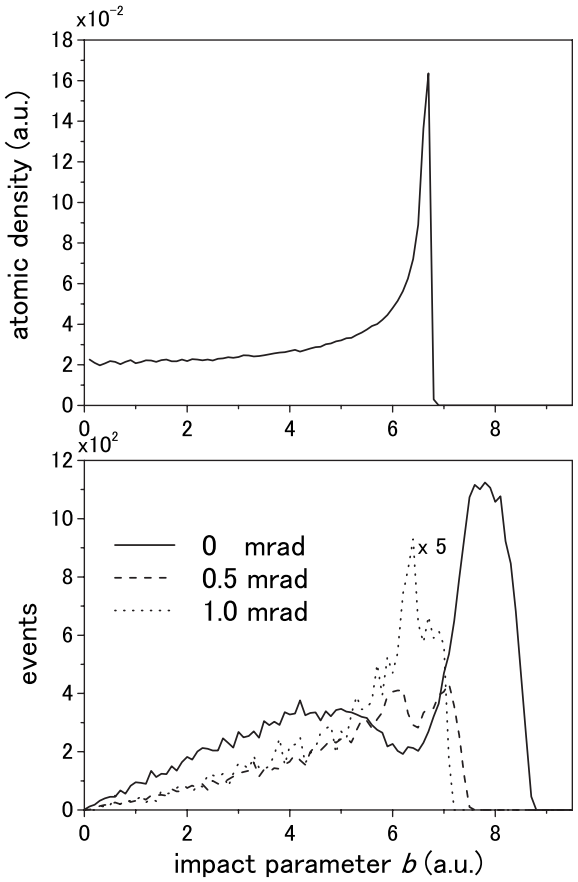

FIG. 2. Calculated scattering yields for θ=0, 0.5, and 1.0 mrad plotted as a function of the impact parameter b measured from the center of C_{60}.

specific fragment ion is produced in equivalent impact parameter collisions independently of the scattering angle. The similar conclusion was also derived in our previous work using 2 MeV Si^{2+} ions [17].

In order to know the most probable impact parameters at which fixed-size specific fragment ions are produced preferentially, we calculated the electronic energy deposition E_d as a function of the impact parameter b, as described below. The calculation was done by using the local density approximation (LDA) [28–30]. The mean electronic energy loss of an incident particle (charge q and velocity v) in an electron gas is given by

$$-\frac{dE}{dx}(r) = \frac{4\pi q^2}{v^2}\rho(r)L(\rho(r),v), \tag{2}$$

where r the position of the incident ion measured from the C_{60} center, $\rho(r)$ the electron density, and L the stopping number. The electron density is given by the following analytical expression [11,31].

$$\rho(r) = 0.146\exp\left(\frac{-(r-6.6)^2}{2.7}\right). \tag{3}$$

As the velocity of 2 MeV C_1^+ ions is larger than the local Fermi velocity defined as $v_F(r)=[3\pi^2\rho(r)]^{1/3}$, L is obtained by

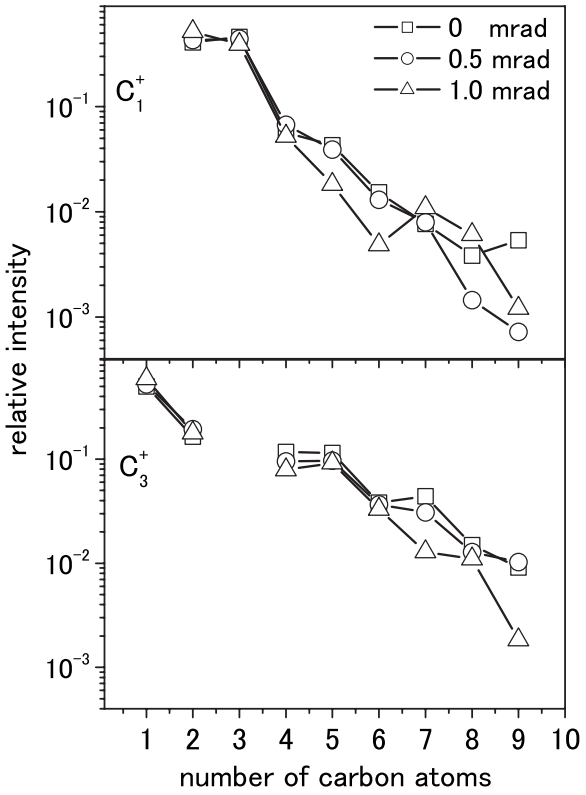

FIG. 3. Relative intensity of fragment ions C_m^+ produced simultaneously with C_1^+ (upper) and C_3^+ (lower) as a function of the cluster size m obtained for 1e-loss collisions of 2 MeV C^+ at scattering angles of θ=0, 0.5, and 1.0 mrad.

$$L(\rho(r),v) = \ln\left(\frac{2v^2}{\omega_p(r)}\right) - \frac{3}{5}\left(\frac{v_F(r)}{v}\right)^2, \tag{4}$$

with the plasma frequency $\omega(r)=[4\pi\rho(r)]^{1/2}$. The mean energy deposition E_d for a certain impact parameter b is obtained by a linear integral of Eq. (2) along the beam trajectory as

$$E_d(b) = \frac{4\pi q^2}{v^2}\int_{-\infty}^{\infty}\rho(r)L(\rho(r),v)dz. \tag{5}$$

In calculations, we used instead of q an effective charge obtained from [32].

Calculated results of E_d are presented in Fig. 5 as a function of b. The value of E_d reaches about 800 eV in the peripheral area of C_{60}, and its average value is about 600 eV. As we discussed in detail in [7,16,17], the total energy deposition E_d is shared by ionization and internal excitation with a certain partition rate. Therefore once the degree of ionization (r) is known, the value of E_d may be deduced separately for each fragment ion. As for partition rates, we used theoretical values reported for other collision systems of $0.2-10^4$ keV $H+H_2O$ [33] and 1.4 MeV/amu $U^{32+}+Ne$ [34]. According to these papers, about 20% of E_d is spent for internal excitation and 80% for ionization energy [33], and 75% of the ionization energy is carried away by ionized electrons as their kinetic energies [34]. The rest of the ionization energy ($E_d\times0.8\times0.25=E_d\times0.2$) equals a sum of ionization

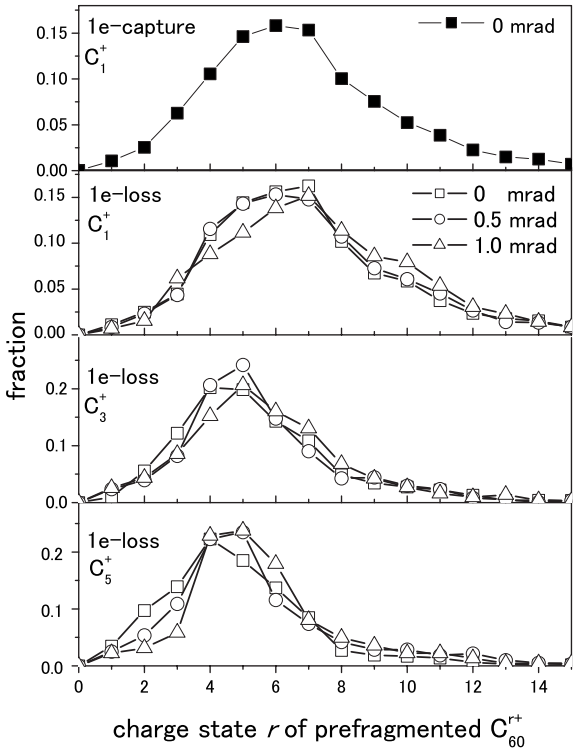

FIG. 4. Charge state distribution correlated with specific fragment ions C_m^+ in single electron loss collisions of 2 MeV C^+ at scattering angles of θ=0, 0.5, and 1.0 mrad.

potentials of all the ionized electrons. Hence E_d is related to the degree of ionization as

$$E_d \times 0.2 = \sum_{i=1}^{r} I_i, \tag{6}$$

where I_i is the ith ionization potential given by I_i=3.77 +3.82i [3]. As for C_1^+, for instance, E_d is calculated to be 665 eV by using an average value of $\bar{r}$=7 obtained from r-distributions as shown in Fig. 4. In this way, we obtained total energy depositions E_d for each fragment ions and plotted them in Fig. 5. We find that C_1^+ is predominantly produced at impact parameters of 5–7 a.u. (cage penetration) and medium size ions C_m^+ (m=5–8) are produced at about 8 a.u. These results are consistent with those obtained from scattering angle measurements described above.

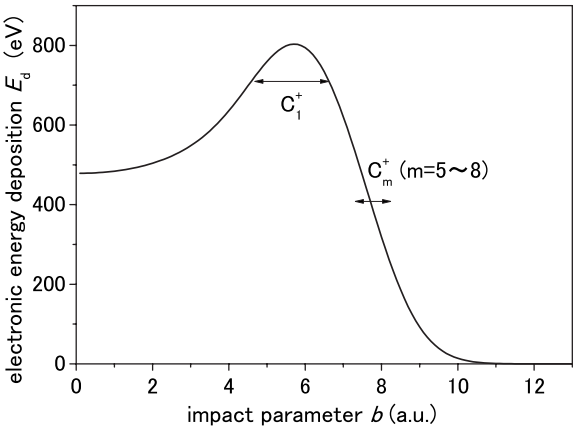

FIG. 5. Electronic energy deposition E_d into a C_{60} by 2 MeV C^+ as a function of the impact parameter b. The most probable impact parameters for the production of C_1^+ and C_m^+ are also shown by arrows.

In summary, collision-induced C_{60} fragmentation following charge exchange of 2 MeV C^+ ions scattered into small forward angles has been investigated. It was found that the charge-state distribution of prefragmented C_{60}^{r+} ions correlated with fixed-size fragment ions C_m^+ is essentially independent of both scattering angle and projectile final charge. This characteristic was also found for mass distributions of correlated fragment ion pairs. It implies evidently that fixed-size fragment ions are produced in equivalent impact parameter collisions independently of the projectile scattering angle.

We attempted calculations to determine the most probable impact parameters for the production of specific fragment ions by using an energy partition model. Present experimental results can be reasonably interpreted by our simple calculations. It should be noted, however, that the charge-state distributions are spread widely and it needs more accurate statistical analysis to achieve more realistic understanding of fragmentation mechanism.

ACKNOWLEDGMENTS

This work was supported by a Grant-in-Aid for Scientific Research (B) No. 16360474 from the Japan Society for the Promotion of Science. We gratefully acknowledge K. Yoshida, K. Norizawa, T. Oka, and H. Nanki for their technical support during the experiment.

[1] E. E. B. Campbell and E. Rohmund, Rep. Prog. Phys. **63**, 1061 (2000).
[2] P. Scheier and T. D. Märk, Phys. Rev. Lett. **73**, 54 (1994).
[3] H. Steger, J. Holzapfel, A. Hielscher, W. Kamke, and I. V. Hertel, Chem. Phys. Lett. **234**, 455 (1995).
[4] V. R. Bhardwaj, P. B. Corkum, and D. M. Rayner, Phys. Rev. Lett. **91**, 203004 (2003).
[5] B. Walch, C. L. Cocke, R. Voelpel, and E. Salzborn, Phys. Rev. Lett. **72**, 1439 (1994).
[6] S. Martin, L. Chen, A. Denis, R. Bredy, J. Bernard, and J. Désesquelles, Phys. Rev. A **62**, 022707 (2000).
[7] H. Tsuchida, A. Itoh, Y. Nakai, K. Miyabe, and N. Imanishi, J. Phys. B **31**, 5383 (1998).
[8] A. Itoh, H. Tsuchida, T. Majima, and N. Imanishi, Phys. Rev. A **59**, 4428 (1999).
[9] J. Opitz *et al.*, Phys. Rev. A **62**, 022705 (2000).
[10] O. Hadjar, P. Földi, R. Hoekstra, R. Morgenstern, and T. Schlathölter, Phys. Rev. Lett. **84**, 4076 (2000).

[11] O. Hadjar, R. Hoekstra, R. Morgenstern, and T. Schlathölter, Phys. Rev. A **63**, 033201 (2001).
[12] A. Reinköster, U. Werner, N. M. Kabachinik, and H. O. Lutz, Phys. Rev. A **64**, 023201 (2001).
[13] A. Itoh, H. Tsuchida, K. Miyabe, T. Majima, and Y. Nakai, Phys. Rev. A **64**, 032702 (2001).
[14] A. Itoh and T. Majima, Vacuum **73**, 53 (2004).
[15] T. Majima, Ph.D. thesis, 2004 (unpublished).
[16] T. Majima, Y. Nakai, H. Tsuchida, and A. Itoh, Phys. Rev. A **69**, 031202(R) (2004).
[17] T. Majima, Y. Nakai, T. Mizuno, H. Tsuchida, and A. Itoh, Phys. Rev. A **74**, 033201 (2006).
[18] T. Mizuno, T. Majima, Y. Nakai, H. Tsuchida, and A. Itoh, Nucl. Instrum. Methods Phys. Res. B **256**, 101 (2007).
[19] U. Thumm, J. Phys. B **27**, 3515 (1994).
[20] U. Thumm, A. Bárány, H. Cederquist, L. Hägg, and C. J. Setterlind, Phys. Rev. A **56**, 4799 (1997).
[21] B. Walch, U. Thumm, M. Stöckli, C. L. Cocke, and S. Klawikowski, Phys. Rev. A **58**, 1261 (1998).
[22] L. Hägg, A. Bárány, H. Cederquist, and U. Thumm, Phys. Scr., T **T80**, 205, (1999).
[23] H. Cederquist *et al.*, Phys. Rev. A **61**, 022712 (2000).
[24] J. P. Desclaux, At. Data Nucl. Data Tables **12**, 311 (1973).
[25] A. Itoh, K. Nose, Y. Hamamoto, T. Mizuno, and K. Ishii, Phys. Rev. A **72**, 052718 (2005).
[26] W. Eckstein, *Computer Simulation of Ion-Solid Interactions* (Springer, Berlin, 1991).
[27] P. L. Grande and G. Schiwietz, Phys. Rev. A **58**, 3796 (1998).
[28] J. Lindhard and M. Scharff, Mat. Fys. Medd. K. Dan. Vidensk. Selsk. **27**, No. 15 (1953).
[29] N. M. Kabachnik, V. N. Kondratyev, Z. Roller-Lutz, and H. O. Lutz, Phys. Rev. A **56**, 2848 (1997).
[30] P. Moretto-Capelle, D. Bordenave-Montesquieu, A. Rentenier, and A. Bordenave-Montesquieu, J. Phys. B **34**, L611 (2001).
[31] M. J. Puska and R. M. Nieminen, Phys. Rev. A **47**, 1181 (1993).
[32] W. Brandt and M. Kitagawa, Phys. Rev. B **25**, 5631 (1982).
[33] J. H. Miller and A. E. S. Green, Radiat. Res. **54**, 343 (1973).
[34] R. E. Olson, J. Ullrich, and H. Schmidt-Böcking, Phys. Rev. A **39**, 5572 (1989).